

Shadow Higgs from a scale-invariant hidden $U(1)_s$ model

We-Fu Chang*

Department of Physics, National Tsing-Hua University, Hsinchu 300, Taiwan

John N. Ng[†] and Jackson M. S. Wu[‡]

Theory group, TRIUMF, 4004 Wesbrook Mall, Vancouver, B.C., Canada

(Dated: May 16, 2018)

Abstract

We study a scale invariant $SU(2) \times U(1)_Y \times U(1)_s$ model which has only dimensionless couplings. The shadow $U(1)_s$ is hidden, and it interacts with the Standard Model (SM) solely through mixing in the scalar sector and kinetic mixing of the $U(1)$ gauge bosons. The gauge symmetries are broken radiatively by the Coleman-Weinberg mechanism. Lifting of the flat direction results in a light shadow Higgs or “scalón”, and a heavier scalar which we identify as the SM Higgs boson. The phenomenology of this model is discussed. It is possible that shadow Higgs boson can be discovered in precision t -quark studies at the LHC. The conditions that it be a dark matter candidate is also discussed.

*Electronic address: wfchang@phys.nthu.edu.tw

†Electronic address: misery@triumf.ca

‡Electronic address: jwu@triumf.ca

I. INTRODUCTION

There has been much recent interest in the idea of Standard Model (SM) having a hidden sector wherein the matter content are SM gauge singlets, but transform non-trivially according to the hidden sector gauge groups [1, 2, 3, 4, 5, 6, 7, 8, 9, 10]. Hidden sectors arise in many top-down models, including those inspired by the brane world scenario and string theory. Most discussion of them posit an association with a very high mass scale, and their couplings to the visible SM sector are often through nonrenormalizable or loop effects. This need not be the case however, and it has been noticed that through renormalizable interactions, the hidden sector can be probed at energies soon to be available at the Large Hadron Collider (LHC).

We consider here a simple case where the hidden sector contains a single complex scalar gauged under an additional $U(1)$ to the hypercharge of the SM. Such a $U(1)$ factor is ubiquitous in gauge theories as it forms a part of a more complicated gauge group. Thus, we expect the physics we explore in this paper would be generic across a variety of models.

There are two gauge-invariant (and renormalizable) ways the $U(1)$ gauged hidden sector can communicate with the SM fields. One is through kinetic mixing between the field strengths of the SM $U(1)_Y$ and our hidden sector “shadow” $U(1)_s$. In older constructions where the extra gauge sector couples directly to the SM fermions, this leads to the well-known Z' physics [11]. In the hidden sector context, there is no direct coupling, and the phenomenological impact of the gauge mixing between $U(1)_Y$ and $U(1)_s$ has been studied in [12, 13, 14, 15]. The other way is through mixing between the SM Higgs with the hidden sector scalar, the “shadow Higgs” ϕ_s . In this paper we examine the phenomenology of this Higgs mixing in a complete model.

Motivated by the anticipated start up of LHC, models studying the modifications of the SM Higgs signal due to an extended Higgs sector uncharged under the SM gauge group have been proposed (see e.g. [5, 16]). The additional scalars are often constructed to be heavier (if not very much so) than the SM Higgs to avoid the current bounds from electroweak precision tests (EWPTs). But with a hidden sector construction, this need not be so. Indeed, if the hidden sector scalars are very light ($\lesssim 100 \mathcal{O}(\text{MeV})$), they can be candidates for dark matter [17] (under suitable assumptions).

With this in mind, we focus in this paper on a special case of the renormalizable model

given in [15] where it is classically conformal invariant, and the symmetry breaking is induced radiatively via Coleman-Weinberg (CW) mechanism [18]¹. Besides its elegance, the occurrence of a small mass scale through CW mechanism is a natural consequence of the conformal symmetry breaking. This feature precluded the implementation of CW mechanism in a SM context because the prediction of the Higgs mass there ($\lesssim 10$ GeV) is far lower than the current lower bound of 114.4 GeV at 95% CL from direct searched at LEP2 [20]. But in terms of our hidden $U(1)_s$ model with its one extra scalar, the same feature becomes key in ensuring in addition to a SM-like Higgs boson, a light shadow Higgs, which is not only viable under the current EWPT constraints, it also generates a new signal in the top decays testable at the LHC. In analyzing our model, we apply the methods of Gildener and S. Weinberg (GW) [21] which allows perturbation theory to be used in a CW context with multiple scalars.

The organization of our paper is as follows. In the next section, we review the work of GW to set up the framework. In Sec. III we apply the methods of GW to our model and calculate the mass of the scalar bosons. In Sec. IV, we discuss the phenomenology of the scalar sector of our model. We summarize in Sec. V.

II. REVIEW OF GW RESULTS

In this section, we review the main idea of the GW analysis, and we record useful formulae from that work to set up the framework from which we apply to our model. We will follow Ref. [21] closely below.

The work of GW is the earliest comprehensive study of the effective potential that extended the analysis of CW to massless field theories with multiple scalar fields. They considered a renormalizable gauge theory with an arbitrary multiplet of real scalar fields Φ_i . The tree level potential is given by

$$V_0(\Phi) = \frac{1}{24} f_{ijkl} \Phi_i \Phi_j \Phi_k \Phi_l. \quad (1)$$

Typically, the nonzero components of f_{ijkl} are of order e^2 , where $e \ll 1$ stands for the generic

¹ Similar ideas has previously been applied in the context of grand unified theory resulting in a different phenomenology [19]. CW mechanism in a hidden sector context have recently also been applied in the dynamical generation of the neutrino mass [9] and the electroweak phase transition [10].

gauge couplings in the theory.

To ensure that perturbation theory will stay valid throughout the analysis, the prescription of GW is to choose a value Λ_W of the renormalization scale Λ , at which $V_0(\Phi)$ has a nontrivial minimum on some ray $\Phi_i = N_i \phi$, where \mathbf{N} is a unit vector in the field space and ϕ is the radial distance from the origin of the field space. This prescription is implemented by adjusting Λ so that

$$\min_{N_i N_i=1} V_0(\mathbf{N}) = \min_{N_i N_i=1} f_{ijkl} N_i N_j N_k N_l = 0. \quad (2)$$

Note that this imposes only a *single* constraint on the f_{ijkl} . One cannot choose a renormalization scale such that all f_{ijkl} vanish, just a single combination.

Suppose the minimum (2) is attained for some specific unit vector $N_i = n_i$. Then one necessary condition is that of the stationary point

$$\left. \frac{\partial V_0(\mathbf{N})}{\partial N_i} \right|_{\mathbf{n}} = 0 \iff f_{ijkl} n_j n_k n_l = 0. \quad (3)$$

For $V_0(\mathbf{N})$ to attain a minimum at $\mathbf{N} = \mathbf{n}$ further requires that for all vectors \mathbf{u}

$$P_{ij} u_i u_j \geq 0, \quad P_{ij} \equiv \left. \frac{\partial^2 V_0(\mathbf{N})}{\partial N_i \partial N_j} \right|_{\mathbf{n}} = \frac{1}{2} f_{ijkl} n_k n_l, \quad (4)$$

i.e. the eigenvalues of P are either positive or zero .

Turning on the higher-order corrections δV in the potential will give rise to a small curvature in the radial direction, which picks out a definite value v of ϕ at the minimum, as well as causing a small shift in the direction of the ray Φ_i at this minimum. The stationary point condition at the new, perturbed minimum $\mathbf{n}v + \delta\Phi$ is

$$0 = \left. \frac{\partial}{\partial \Phi_i} (V_0(\Phi) + \delta V(\Phi)) \right|_{\mathbf{n}v + \delta\Phi}, \quad (5)$$

or to first order in small quantities

$$0 = P_{ij} \delta\Phi_j v^2 + \left. \frac{\partial \delta V(\Phi)}{\partial \Phi_i} \right|_{\mathbf{n}v}. \quad (6)$$

This uniquely determines $\delta\Phi$ except for possible terms in directions along eigenvectors of P with eigenvalue zero, which includes \mathbf{n} by construction

$$P_{ij} n_j = \left. \frac{1}{2} \frac{\partial V_0(\mathbf{N})}{\partial N_i} \right|_{\mathbf{n}} = 0, \quad (7)$$

and the Goldstone modes $\Theta_\alpha \mathbf{n}$ corresponding to the continuous symmetries Θ_α . There is no reason, in general, to expect any other eigenvectors of P with zero eigenvalues, and is assumed so.

Instead of using (6) to determine $\delta\Phi$, contracting (6) with n_i and using (7) leads to a basic equation that determines the value of v

$$0 = \frac{\partial}{\partial \Phi_i} \delta V(\Phi) \Big|_{\mathbf{n}v} = \frac{\partial}{\partial \phi} \delta V(\mathbf{n}\phi) \Big|_v. \quad (8)$$

Calculating δV to one-loop, the potential along the ray $\Phi = \mathbf{n}\phi$ can be written in the form

$$\delta V(\mathbf{n}\phi) = A \phi^4 + B \phi^4 \log \frac{\phi^2}{\Lambda_W^2}, \quad (9)$$

where A and B are dimensionless constants

$$A = \frac{1}{64\pi^2 v^4} \left\{ 3\text{Tr} \left[M_V^4 \log \frac{M_V^2}{v^2} \right] + \text{Tr} \left[M_S^4 \log \frac{M_S^2}{v^2} \right] - 4\text{Tr} \left[M_F^4 \log \frac{M_F^2}{v^2} \right] \right\} \quad (10)$$

$$B = \frac{1}{64\pi^2 v^4} (3\text{Tr} M_V^4 + \text{Tr} M_S^4 - 4\text{Tr} M_F^4). \quad (11)$$

The trace is over all internal degrees of freedom, and $M_{V,S,F}$ are the zeroth-order vector, scalar, and spinor mass matrices respectively, for a scalar field vacuum expectation value $\mathbf{n}v$.

From (9), the stationary point condition (8) implies

$$\log \frac{v^2}{\Lambda_W^2} = -\frac{1}{2} - \frac{A}{B}. \quad (12)$$

Because of the choice of the renormalization scale (2), both A and B are of order e^4 , so the logarithm is of order unity, and perturbation theory should be valid. Note that this implies Λ_W and v are of the same order.²

The squared masses of the scalar bosons are given by the eigenvalues of the second derivative matrix of the effective potential

$$(M^2)_{ij} = (M_0^2 + \delta M^2)_{ij} = \frac{\partial^2}{\partial \Phi_i \partial \Phi_j} [V_0(\Phi) + \delta V(\Phi)] \Big|_{\mathbf{n}v + \delta\Phi}, \quad (13)$$

where

$$(M_0^2)_{ij} = \frac{\partial^2 V_0(\Phi)}{\partial \Phi_i \partial \Phi_j} \Big|_{\mathbf{n}v} = P_{ij} v^2, \quad (14)$$

² See [21] for more details.

is the zeroth order scalar mass-squared matrix, and

$$(\delta M^2)_{ij} = \frac{\partial^2 \delta V(\Phi)}{\partial \Phi_i \partial \Phi_j} \Big|_{\mathbf{n}v} + f_{ijkl} n_k \delta \Phi_l v, \quad (15)$$

to first order in small quantities, with $\delta \Phi$ determined from (6).

From the discussion above, M_0^2 has a set of positive-definite eigenvalues of order $e^2 v^2$ corresponding to Higgs bosons, plus a set of zero eigenvalues with eigenvectors $\Theta_\alpha \mathbf{n}$ corresponding to Goldstone bosons, plus one zero eigenvalue with eigenvector \mathbf{n} , the ‘‘scalon’’. Provided that δV has the same symmetries as V_0 and is a small perturbation, the Higgs boson mass would remain positive-definite, and the Goldstone bosons would remain massless.

The scalon is a pseudo-Goldstone boson arising from the spontaneous symmetry breaking of the conformal symmetry. Its mass can be straightforwardly calculated from first-order perturbation theory

$$m_s^2 = n_i n_j (\delta M^2)_{ij} = n_i n_j \frac{\partial^2 \delta V(\Phi)}{\partial \Phi_i \partial \Phi_j} \Big|_{\mathbf{n}v} = \frac{\partial^2}{\partial \phi^2} \delta V(\mathbf{n}\phi) \Big|_{\mathbf{v}}. \quad (16)$$

From (9) and (12), this gives

$$m_s^2 = 8B v^2. \quad (17)$$

III. THE CONFORMAL SHADOW MODEL AND ITS BREAKING

The complete Lagrangian of our model takes the form [15]

$$\mathcal{L} = \mathcal{L}_{SM} - \frac{1}{4} X^{\mu\nu} X_{\mu\nu} - \frac{\epsilon}{2} B^{\mu\nu} X_{\mu\nu} + \left| \left(\partial_\mu - \frac{1}{2} g_s X_\mu \right) \phi_s \right|^2 - V_0(\Phi, \phi_s). \quad (18)$$

We consider here an initially scale-invariant theory in which the tree level scalar potential is given by

$$V_0(\Phi, \phi_s) = \lambda (\Phi^\dagger \Phi)^2 + \lambda_s (\phi_s^* \phi_s)^2 + 2\kappa (\Phi^\dagger \Phi) (\phi_s^* \phi_s). \quad (19)$$

We assume that the quartic coupling constants λ , λ_s , and κ are all of order at least g_s^2 , where $g_s \ll 1$ is the gauge coupling constant of the shadow $U(1)_s$.

In unitary gauge, the scalar fields on some ray $\varphi_i = \rho N_i$, where \mathbf{N} is a unit vector in the field space $\{\Phi \otimes \phi_s\}$, can be parameterized as

$$\Phi = \frac{\rho}{\sqrt{2}} \begin{pmatrix} 0 \\ N_1 \end{pmatrix}, \quad \phi_s = \frac{\rho}{\sqrt{2}} N_2. \quad (20)$$

In terms of these coordinates, the tree level potential has the form

$$V_0(\boldsymbol{\varphi}) = V_0(\rho, \mathbf{N}) = \frac{\rho^4}{4}(\lambda N_1^4 + \lambda_s N_2^4 + 2\kappa N_1^2 N_2^2). \quad (21)$$

We assume that λ and λ_s are positive so that the potential is bounded below.

The GW condition (2) and (3) that V_0 attains a minimum value of zero on a unit sphere for some unit vector $\mathbf{N} = \mathbf{n}$ implies that

$$\left. \frac{\partial V_0}{\partial N_i} \right|_{\mathbf{n}} = 0, \quad V_0|_{\mathbf{n}} = 0. \quad (22)$$

The solution of these equations is given by

$$n_1^2 = \frac{\sqrt{\lambda_s}}{\sqrt{\lambda} + \sqrt{\lambda_s}}, \quad n_2^2 = \frac{\sqrt{\lambda}}{\sqrt{\lambda} + \sqrt{\lambda_s}}, \quad \kappa = -\sqrt{\lambda\lambda_s}. \quad (23)$$

The first two relations specify the direction of the unperturbed minimum of the zeroth-order potential V_0 ; the last relation is a consistency condition that V_0 vanishes along this direction.

Along the ray $\varphi_i = n_i \rho$, the one-loop effective potential is given by

$$V_{1L}(\mathbf{n}\rho) = A \rho^4 + B \rho^4 \log \frac{\rho^2}{\Lambda_W^2}, \quad (24)$$

where

$$A = \frac{1}{64\pi^2 v^4} \left\{ 6m_W^4 \log \frac{m_W^2}{v^2} + 3m_{Z_1}^4 \log \frac{m_{Z_1}^2}{v^2} + 3m_{Z_2}^4 \log \frac{m_{Z_2}^2}{v^2} + m_{H,0}^4 \log \frac{m_{H,0}^2}{v^2} - 12m_t^4 \log \frac{m_t^2}{v^2} \right\}, \quad (25)$$

$$B = \frac{1}{64\pi^2 v^4} (6m_W^4 + 3m_{Z_1}^4 + 3m_{Z_2}^4 + m_{H,0}^4 - 12m_t^4). \quad (26)$$

Note that we have included only the t -quark contribution since it overwhelms all other fermionic contributions.

The mass of the vector bosons at tree level are given by

$$\begin{aligned} m_W^2 &= \frac{1}{4} g_W^2 n_1^2 v^2 = \frac{1}{4} g_W^2 v_r^2, \quad (27) \\ m_{Z_{1,2}}^2 &= \frac{v^2}{8} \left\{ n_1^2 \left[g_W^2 + g_Y^2 (1 + s_\epsilon^2) \right] + c_\epsilon^2 n_2^2 g_s^2 \right. \\ &\quad \left. \mp \sqrt{4 c_\epsilon^2 s_\epsilon^2 n_1^2 n_2^2 g_Y^2 g_s^2 + \left[n_1^2 (g_W^2 + g_Y^2 (1 + s_\epsilon^2)) - c_\epsilon^2 n_2^2 g_s^2 \right]^2} \right\} \\ &= \frac{v_r^2}{8} \left\{ g_s(r, \epsilon)^2 + g_W^2 + g_Y^2 (1 + s_\epsilon^2) \right. \\ &\quad \left. \mp \sqrt{4 s_\epsilon^2 g_Y^2 g_s(r, \epsilon)^2 + \left[g_W^2 + g_Y^2 (1 + s_\epsilon^2) - g_s(r, \epsilon)^2 \right]^2} \right\}, \quad (28) \end{aligned}$$

where ³

$$s_\epsilon = \frac{\epsilon}{\sqrt{1+\epsilon^2}}, \quad c_\epsilon = \frac{1}{\sqrt{1+\epsilon^2}}, \quad (29)$$

and we have defined

$$r \equiv \frac{\sqrt{\lambda}}{\sqrt{\lambda_s}}, \quad v_r \equiv n_1 v = \frac{v}{\sqrt{1+r}}, \quad g_s(r, \epsilon) \equiv c_\epsilon \sqrt{r} g_s. \quad (30)$$

Note that we work in the mass-diagonal basis where the gauge kinetic terms are in canonical form, and these are the gauge bosons in that basis.

The mass of the scalar boson at tree level is given by

$$m_{H,0}^2 = 2\sqrt{\lambda\lambda_s} v^2. \quad (31)$$

There is only one heavy Higgs boson in our model that has a tree level mass which is given $m_{H,0}$. The only other massive scalar boson is the scalon, but it has no tree level mass. The scalon gets its mass purely from radiative processes through CW mechanism, and is light. From (26), (27), (28), and (31), the scalon mass as defined in (17), is given by

$$\begin{aligned} m_s^2 &= 8B v^2 \\ &= \frac{3v_r^2}{64\pi^2(1+r)} \left[\frac{3g_W^4}{2} + g_Y^2 g_W^2 (1+s_\epsilon^2) + \frac{g_Y^4}{2} (1+s_\epsilon^2)^2 + s_\epsilon^2 g_Y^2 g_s(r, \epsilon)^2 + \frac{g_s(r, \epsilon)^4}{2} \right] \\ &\quad + \frac{v_r^2}{2\pi^2} (1+r) \kappa^2 - \frac{3m_t^4}{2\pi^2 v_r^2 (1+r)}. \end{aligned} \quad (32)$$

After spontaneous breaking of conformal symmetry by the CW mechanism, we can write the scalar fields as

$$\Phi = \frac{1}{\sqrt{2}} \begin{pmatrix} 0 \\ n_1 v + h \end{pmatrix}, \quad \phi_s = \frac{1}{\sqrt{2}} (n_2 v + s), \quad (33)$$

where h and s are the excitations about the minimum along directions n_1 and n_2 respectively.

From (19), the tree level potential V_0 then takes the form

$$\begin{aligned} V_0(\Phi, \phi_s) &= \frac{\lambda}{4} h^4 + \lambda n_1 v h^3 + \kappa \left(n_2 v h^2 s + \frac{1}{2} h^2 s^2 + n_1 v h s^2 \right) + \lambda_s n_2 v s^3 + \frac{\lambda_s}{4} s^4 \\ &\quad + \frac{v^2}{2} (3n_1^2 \lambda + n_2^2 \kappa) h^2 + 2\kappa n_1 n_2 v^2 h s + \frac{v^2}{2} (n_1^2 \kappa + 3n_2^2 \lambda_s) s^2, \end{aligned} \quad (34)$$

with the linear terms vanish by (23).

³ The signs here correct the typographical error in the definition of the same quantities in [15].

The physical mass-diagonal basis is defined by

$$\begin{pmatrix} h \\ s \end{pmatrix} = U \begin{pmatrix} H_1 \\ H_2 \end{pmatrix} = \begin{pmatrix} n_1 H_1 - n_2 H_2 \\ n_2 H_1 + n_1 H_2 \end{pmatrix}, \quad (35)$$

where U is an orthogonal matrix given by

$$U = \begin{pmatrix} n_1 & -n_2 \\ n_2 & n_1 \end{pmatrix} = \begin{pmatrix} \frac{1}{\sqrt{1+r}} & -\frac{\sqrt{r}}{\sqrt{1+r}} \\ \frac{\sqrt{r}}{\sqrt{1+r}} & \frac{1}{\sqrt{1+r}} \end{pmatrix}. \quad (36)$$

Note that the matrix U is exactly the matrix which diagonalize the zeroth order scalar mass matrix M_0^2 as defined in (14) (or equivalently, the matrix P defined in (4)) i.e.⁴

$$\begin{aligned} M_0^2 &= P v^2 = \begin{pmatrix} 3n_1^2 \lambda + n_2^2 \kappa & 2n_1 n_2 \kappa \\ 2n_1 n_2 \kappa & n_1^2 \kappa + 3n_2^2 \lambda_s \end{pmatrix} v^2 \\ &= U^{-1} \begin{pmatrix} m_{H_1}^2 & 0 \\ 0 & m_{H_2}^2 \end{pmatrix} U = U^{-1} \begin{pmatrix} 0 & 0 \\ 0 & 2\sqrt{\lambda \lambda_s} \end{pmatrix} U v^2. \end{aligned} \quad (37)$$

We see thus that H_1 corresponds to the scalon state, and H_2 corresponds to the heavy Higgs boson state.

Going to the physical basis, we get with the help of (23) and (30)

$$\begin{aligned} V_0(\Phi, \phi_s) &= \frac{m_{H,0}^2}{2} H_2^2 - \sqrt{\frac{\lambda}{2}} \left(1 - \frac{1}{r}\right) m_{H,0} H_2^3 + \frac{\lambda}{4} \left(1 - \frac{1}{r}\right)^2 H_2^4 \\ &\quad - \kappa H_1^2 H_2^2 - 2\kappa \sqrt{1+r} v_r H_1 H_2^2 - \sqrt{\lambda |\kappa|} \left(1 - \frac{1}{r}\right) H_1 H_2^3. \end{aligned} \quad (38)$$

Note that from (23), $\kappa < 0$ since $\lambda, \lambda_s > 0$. The Feynman rules in the scalar sector of our model can be readily read off from (38).

Notice in (38) quartic terms contain no more than two scalon (H_1) fields, and in cubic terms no more than one. This is a general feature of the GW framework that follows from the stationary point condition (3): Recall the general form of the tree level potential (1). After symmetry breaking, the scalar field takes the form

$$\Phi_i = n_i v + \varphi_i = n_i v + (U \cdot \mathbf{H})_i, \quad (U \cdot \mathbf{H})_i = \sum_j \zeta_j H_j, \quad (39)$$

⁴ Because of our choice of the unitary gauge (20) rotated away all gauge degrees of freedom, M_0^2 will contain no zero eigenvalues corresponding to Goldstone bosons.

where φ_i are the excitations about the minimum in the i -th direction, and ζ_i are the eigenvectors of the mass matrix M_0^2 . By construction, the flat direction \mathbf{n} is always an eigenvector of M_0^2 (see discussion above). Thus, since the scalon is by definition the state associated with \mathbf{n} , the statement follows.

IV. CONSTRAINTS AND PHENOMENOLOGY

The parameters relevant for the scalar sector in our model are the gauge kinetic mixing angle s_ϵ , the gauge coupling g_s , the quartic couplings λ , λ_s , κ , and the scalar field vacuum expectation value v . Because of relations (23) and (30), we will trade in λ_s and v , and use the parameter set $\{s_\epsilon, g_s, \lambda, \kappa, r, v_r\}$ for convenience of analysis below.

From the mass of the W boson (27), and the relation between m_W and the Fermi coupling constant

$$\frac{G_F}{\sqrt{2}} = \frac{g_W^2}{8m_W^2}, \quad (40)$$

v_r can be determined, and it is given by

$$v_r = 2^{-1/4} G_F^{-1/2} = 246.221 \text{ GeV}. \quad (41)$$

Since our interest here is in exploring the parameter space of the scalar sector of our model, given that $s_\epsilon \lesssim 10^{-2}$ (see Ref. [15]), we will neglect higher order corrections in ϵ , and treat s_ϵ as zero in the analysis below ⁵.

Setting $s_\epsilon = 0$, we get from (28)

$$m_{Z_1}^2 = \frac{v_r^2}{4}(g_W^2 + g_Y^2) = m_Z^2, \quad m_{Z_2}^2 = \frac{v_r^2}{4} r g_s^2, \quad (42)$$

i.e., Z_1 is automatically the SM Z , while Z_2 is the shadow Z ⁶. With v_r fixed, we can write r as a function of g_s and m_{Z_2} ($= m_{Z_s}$)

$$r = \frac{4m_{Z_2}^2}{v_r^2} \frac{1}{g_s^2} = \frac{m_{Z_s}^2}{m_W^2} \frac{g_W^2}{g_s^2}. \quad (43)$$

⁵ For the physical, parity-even processes we consider below, the leading corrections start at $\mathcal{O}(\epsilon^2)$. We set $s_\epsilon = 0$ here purely for the purpose of simplifying the analysis; the kinetic mixing parameter ϵ should never be thought of as being identically zero, as then it implies a complete decoupling of the shadow Z from the visible sector that would upset the cosmological bounds. We leave the more complete but also more complicated analysis that kept $s_\epsilon \neq 0$ at leading order to future works [22].

⁶ The convention we adopt is that Z_2 shall always denote the heavier state, viz. the shadow Z . With $s_\epsilon = 0$, this corresponds to taking the negative sign for the square roots in (28).

In Fig 1 and 2, we show the functional interdependencies implied by (43).

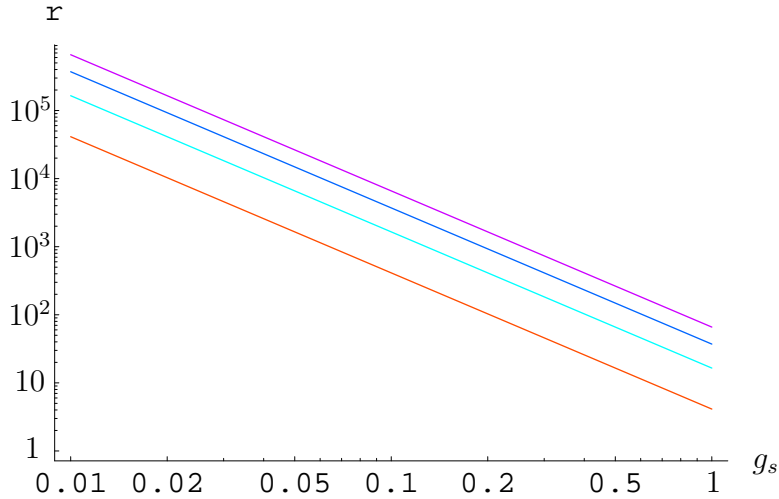


FIG. 1: The parameter r as a function of g_s for m_{Z_s} fixed at 250 (bottom line), 500, 750, and 1000 (top line) GeV.

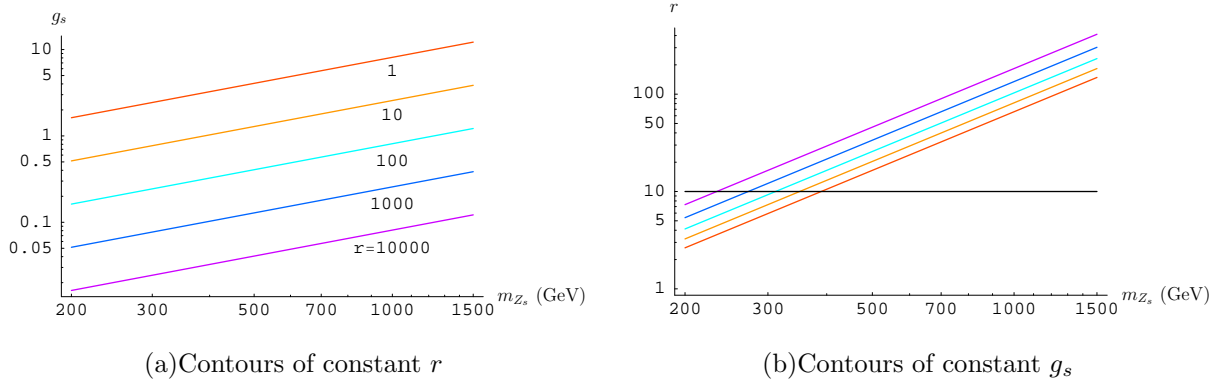


FIG. 2: Relationships between r , g_s , and m_{Z_s} . In (b), the contour lines are for fixed value of $g_s = 1$ (bottom line), 0.9, 0.8, 0.7, and 0.6 (top line).

As is apparent from Eq. (43), Fig. 1 and Fig. 2, for a given value of g_s , the heavier the shadow Z, the larger r needs to be. For example, if $g_s \sim g_W \sim 0.65$, to have $m_{Z_s} > 500$ GeV would require $r > 10^2$, and r would be even larger if g_s is smaller. In Fig. 2(b), each contour line forms a lower bound on the values of r for a given value of g_s . We see from it that if r is of order 10, for $m_{Z_s} > 1$ TeV, g_s would have to exceed its perturbative limit, which we conservatively take to be $g_s = 1$. While for $500 \text{ GeV} < m_{Z_s} < 1 \text{ TeV}$, g_s would have to be close to the unity.

We now turn our attention to the Higgs sector. In contrast to the multiscalar construction

with CW mechanism in a GUT context, we emphasize and reiterate here that it is the heavy scalar boson, H_2 , that will take the role of the SM Higgs boson (with SM Higgs mass) in our model. Being a pseudo-Goldstone boson of the spontaneously broken conformal symmetry, the scalon, H_1 , or the “shadow Higgs” is naturally light, and will not be fine tuned to the electroweak scale such that H_2 becomes sufficiently heavy to escape detection.

Below, we will first map out the parametric dependence of the shadow Higgs mass on g_s , κ and r . Then we will show that a light shadow Higgs is viable from direct search and other experiments, and we give bounds on the parameter space of the shadow Higgs from these experimental constraints. We will show that the shadow Higgs can be very light ($< 2m_e$), and we comment on the possibility of it been a dark matter candidate, and the degree of fine tuning that is required.

A. The mass of shadow Higgs

To one-loop order, the mass of the heavy Higgs boson, m_{H_2} , is given by the largest eigenvalue of the matrix defined in (13). Due to its complexity, we do not give its analytical form here. Rather, we will set m_{H_2} to the SM Higgs mass, and use it as a constraint which we solve numerically for the allowed values of κ to be used as an input to the shadow Higgs mass, m_{H_1} .

With v_r fixed, m_{H_2} depends on the parameters g_s , κ , and r which we trade in for m_{Z_s} using (43). In Fig. 3, we show the dependence of κ on g_s , m_{Z_s} , and m_{H_2} . We see that κ varies as a power of each of the parameters g_s , m_{H_2} , and m_{Z_s} . Note that $|\kappa|$ is at most of order g_s^3 in the range of m_{Z_s} and m_{H_2} we consider. In particular, the magnitude of κ decrease as the value of m_{Z_s} (m_{H_2}) increase (decrease).

With s_ϵ taken to be zero, the shadow Higgs mass (32) takes the form

$$m_{H_1}^2 = \frac{3v_r^2}{64\pi^2(1+r)} \left[\frac{3g_W^4}{2} + g_Y^2 g_W^2 + \frac{g_Y^4}{2} + \frac{g_s^4 r^2}{2} \right] + \frac{v_r^2}{2\pi^2}(1+r)\kappa^2 - \frac{3m_t^4}{2\pi^2 v_r^2(1+r)}. \quad (44)$$

In Fig. 4, we show m_{H_1} as a function of g_s along the contours $r(g_s)$ of constant m_{Z_s} and $\kappa(g_s)$ of constant m_{H_2} . For $g_s \sim g_W \sim 0.65$, we see that the shadow Higgs mass varies from sub GeV range to tens of GeV, depending on m_{Z_s} . Note that m_{H_1} decreases as a positive power of g_s , reflecting the fact that κ^2 decreases faster than $r^{-1} \propto g_s^2$ (see (43)).

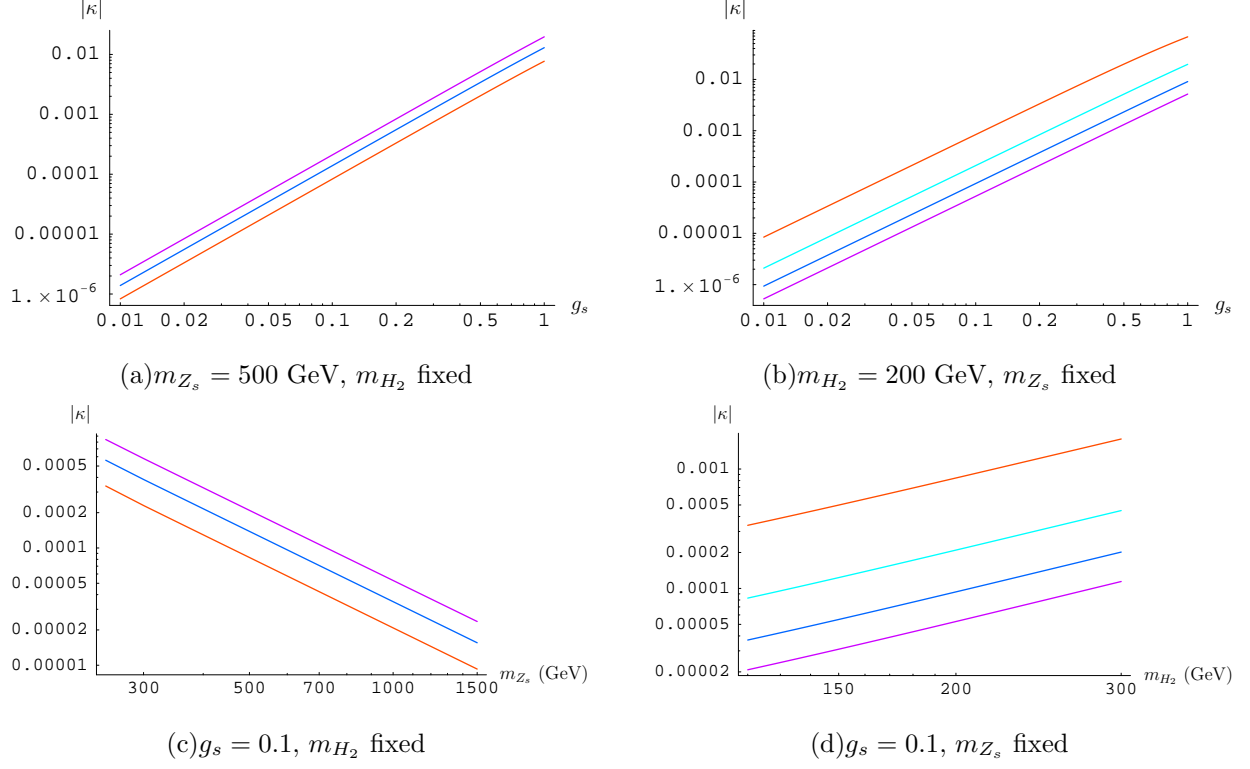


FIG. 3: Contours of $|\kappa|$ as a function of g_s , m_{H_2} , and m_{Z_s} individually. In (a) and (c), m_{H_2} is fixed at 120 (bottom line), 160, and 200 (top line) GeV. In (b) and (d), m_{Z_s} is fixed at 250 (top), 500, 750, and 1000 (bottom) GeV.

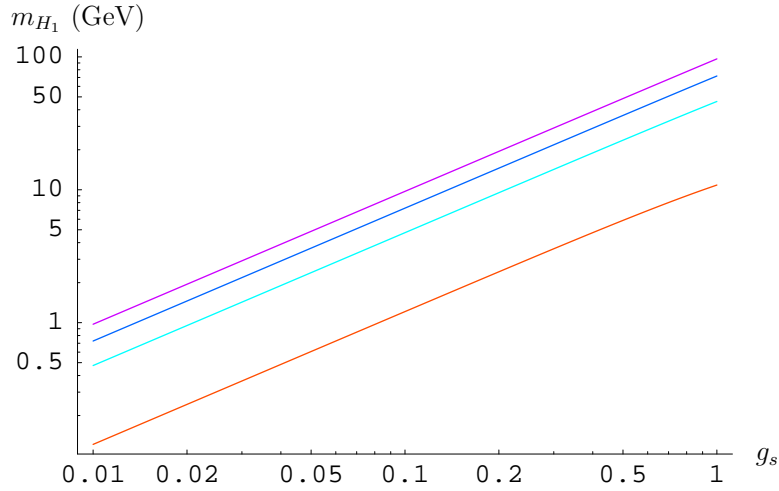


FIG. 4: The mass of shadow Higgs, m_{H_1} , as a function of g_s for $m_{H_2} = 200$ GeV and m_{Z_s} fixed at 250 (bottom line), 500, 750, and 1000 (top line) GeV.

B. Limits form direct LEP search

The shadow Higgs couples to SM fields only through its mixing with the SM Higgs. From (35), one can see that a triple coupling of the form $H_1 FF$, where F is a SM field, is simply that of the SM Higgs scaled by a mixing factor of $n_1 = (1+r)^{-1/2}$. At LEP, an important parameter used in the direct Higgs search is $\xi^2 \equiv (g_{HZZ}/g_{HZZ}^{SM})^2$, where g_{HZZ} denotes the non-standard HZZ coupling and g_{HZZ}^{SM} that in the SM. In terms of our model, the ξ^2 parameter becomes

$$\xi_1^2 = \left(\frac{g_{H_1ZZ}}{g_{HZZ}^{SM}} \right)^2 = \frac{1}{1+r}, \quad \xi_2^2 = \left(\frac{g_{H_2ZZ}}{g_{HZZ}^{SM}} \right)^2 = \frac{r}{1+r}, \quad (45)$$

for the shadow Higgs, H_1 , and the SM-like Higgs, H_2 , respectively.

To see whether or not the shadow Higgs is ruled out at LEP, we can simply apply the LEP bound to ξ_1^2 . The most stringent bound is obtained when the shadow Higgs mass is about 20 GeV, where $\xi_1^2 \lesssim 2 \times 10^{-2}$ [20, 23]; elsewhere the bound is rather weak. From the discussion above, we have $g_{H_1ZZ} < g_{HZZ}^{SM}/10$ for much of the parameter space. Thus the shadow Higgs can easily pass the existing bound from the direct Higgs search.

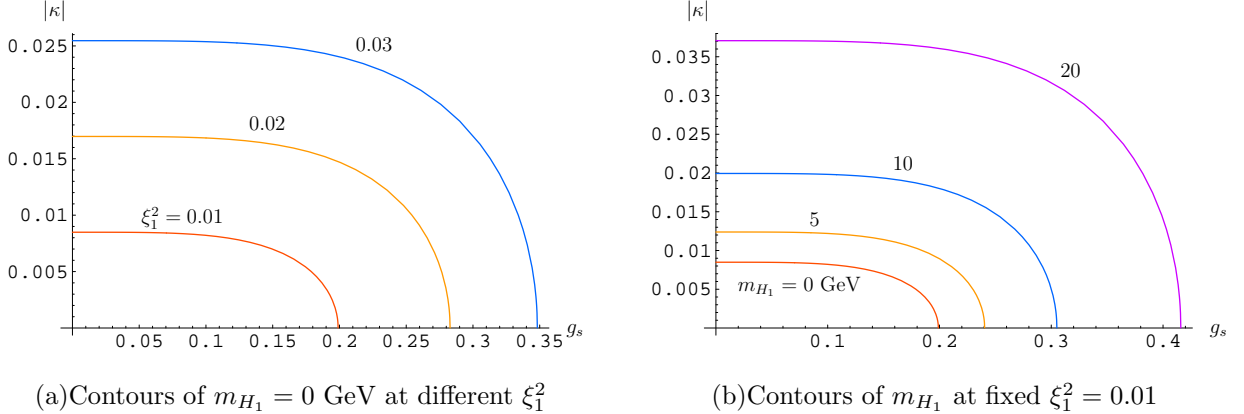


FIG. 5: Contours of m_{H_1} as a function of g_s and κ for fixed values of $\xi_1^2 = (1+r)^{-1}$.

With a light shadow Higgs ($m_{H_1} < m_H^{SM}$) viable, we show in Fig. 5 and Fig. 6 the parameter space that can be constrained by the mass of the shadow Higgs, m_{H_1} , and the ratio of the scalar- Z triple coupling squared, ξ_1^2 . Fig. 5(a) shows that for fixed m_{H_1} , decreasing ξ_1^2 (or equivalently, increasing r) shrinks the contour of constant shadow Higgs mass, while Fig. 5(b) shows that for fixed ξ_1 (r), increasing the value of m_{H_1} expands the contour. Given these, the contours in Fig. 6 forms the upper bound on the allowed values of $\{g_s, \kappa\}$ for each fixed value of m_{H_1} .

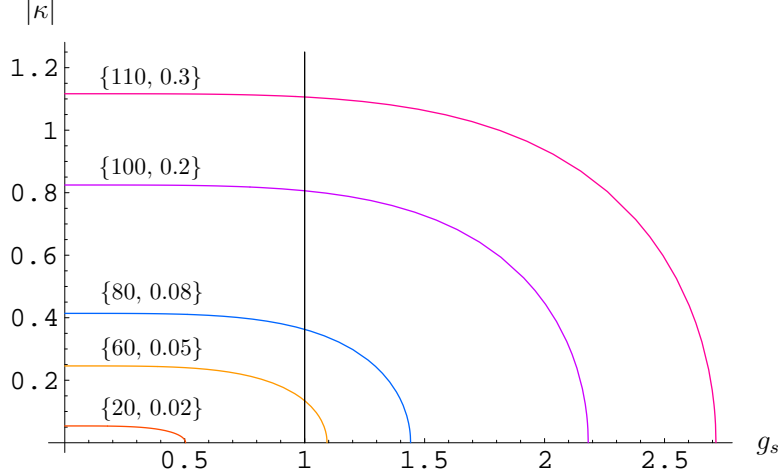


FIG. 6: Contours of m_{H_1} at various $\{m_{H_1} \text{ (GeV)}, \xi_1^2\}$ for ξ_1^2 the maximum value of the LEP 95% CL upper bound found in Ref. [20]. The vertical line marks the boundary for $g_s < 1$.

C. Other limits

The one-loop contribution to muon g-2 from the (neutral) SM Higgs is well known [24]. From (35), scaling it by a factor of $(1+r)^{-1}$ gives the contribution due to the shadow Higgs

$$\Delta a_\mu = \frac{1}{1+r} \frac{G_F m_\mu^2}{4\pi^2 \sqrt{2}} I\left(\frac{m_{H_1}^2}{m_\mu^2}\right), \quad (46)$$

where

$$I(x) = \int_0^1 dy \frac{y^2(2-y)}{(1-y)x + y^2} \sim \begin{cases} \frac{3}{2} - \pi\sqrt{x}, & x \ll 1 \\ \frac{1}{x}(\log x - \frac{7}{6}), & x \gg 1 \\ 0, & x \rightarrow \infty \end{cases}. \quad (47)$$

Thus, for $m_{H_1} > 1$ GeV,

$$\Delta a_\mu \sim \frac{2.5 \times 10^{-11}}{1+r} \left(\frac{\text{GeV}}{m_{H_1}}\right)^2, \quad (48)$$

while for $m_{H_1} \ll m_\mu$, $\Delta a_\mu \sim 3/(1+r) \times 10^{-9}$. Now the latest muon g-2 measurement gives $\Delta a_\mu^{exp} - \Delta a_\mu^{SM} = 2.8(8) \times 10^{-9}$ [25], we see that the shadow Higgs contribution to muon g-2 is at most $(1+r)^{-1}$ of that difference. Giving that $r > 10$ in most of the parameter space, muon g-2 gives no constraint on the shadow Higgs mass.

For a light shadow Higgs with $m_{H_1} \leq 1$ GeV, the most stringent constraint comes from the B meson decays. From comparing the $b \rightarrow s H_1$ penguin diagram to the tree-level

$b \rightarrow cW$ transition, one gets an inclusive branching ratio relation [24]

$$\frac{\Gamma(B \rightarrow H_1 X)}{\Gamma(B \rightarrow e\nu X)} \sim \frac{2.95}{1+r} \left(\frac{m_t}{M_W}\right)^4 \left(1 - \frac{m_{H_1}^2}{m_b^2}\right)^2 \left|\frac{V_{ts}^* V_{tb}}{V_{cb}}\right|^2, \quad (49)$$

where the numerical factor contains the phase space difference of the final state c and s quarks. Taking $Br(B \rightarrow e\nu X) = 0.123$ and $m_{H_1} \ll m_b$, we get

$$Br(B \rightarrow H_1 X) \sim \frac{8}{1+r}. \quad (50)$$

In order to make comparisons with the experimental bound on the exclusive decay modes of the B meson, the shadow Higgs decay branching ratios are needed. However, since the shadow Higgs can decay into light hadrons, the branching ratio calculations involve many hadronic uncertainties. Consider, for example, a shadow Higgs with $m_{H_1} = 500$ MeV that decays mainly into two pions and $\mu^+\mu^-$. With the help of chiral perturbation theory, the branching ratio $Br(H_1 \rightarrow \mu^+\mu^-)$ is estimated to be $\sim 30\%$ [7]. Now if the shadow Higgs is heavier than $2m_K$ or $2m_\tau$, this and the whole decay pattern will change dramatically. Moreover, chiral perturbation may not be reliable anymore in these cases to calculate the decay widths.

From Ref. [26], $Br(B \rightarrow \mu^+\mu^- X) < 3.2 \times 10^{-4}$. Suppose the shadow Higgs decays only into $\mu^+\mu^-$, then a (rather) conservative lower bound on r is given by

$$2 \times 10^4 < r \left(1 - \frac{m_{H_1}^2}{m_b^2}\right)^{-2}. \quad (51)$$

Given this bound, the quarkonium decays branching ratios $Br(J/\Psi \rightarrow H_1\gamma) < 10^{-9}$ and $Br(\Upsilon \rightarrow H_1\gamma) = 1.8 \times 10^{-4}/(1+r) \leq 10^{-8}$, which involve tree-level processes, become insignificant in comparison with $Br(B \rightarrow \mu^+\mu^- X)$, which involves a one-loop process.

D. The case of an extremely light shadow Higgs ($m_{H_1} < 2m_e$)

When the shadow Higgs is lighter than $2m_e$, it decays almost completely into two photons. The corresponding effective interaction can be derived by summing up the contributions from having the t -quark and the W -boson running in the loop, and is given by [24]

$$\Delta\mathcal{L} = \frac{g_{H_1\gamma\gamma}}{4} F^{\mu\nu} F_{\mu\nu} H_1, \quad g_{H_1\gamma\gamma} = \frac{7\alpha}{3\pi v_r(1+r)} \sim \frac{2.2 \times 10^{-5}(\text{GeV})^{-1}}{1+r}, \quad (52)$$

where α is the fine-structure constant.

There is currently no direct experimental bound on the coupling constant $g_{H_1\gamma\gamma}$. The shadow Higgs and one of the two photons in the effective operator can be attached to charged fermions which yield a one-loop contribution to the magnetic moment. However this contribution is buried deep inside the one-loop g-2 contribution discussed above.

The lifetime of the shadow Higgs can be estimated to be

$$\tau_{H_1} \sim (1+r) \left(\frac{68 \text{ keV}}{m_{H_1}} \right)^3 \text{ sec} \sim (1+r) \left(\frac{0.1 \text{ eV}}{m_{H_1}} \right)^3 10^{10} \text{ yr}. \quad (53)$$

For a shadow Higgs lighter than a few tens of keV, its life time may be long enough for it to escape and carry away energy from stars in the horizontal branch with a typical radius of a few tens of light second. Recently, an upper bound on the coupling of a very light exotic spin-0 particle to two photons has been placed at $1.1 \times 10^{-10} \text{ GeV}^{-1}$ by the CAST Collaboration [27]. Applying this bound to the scalar case (53) implies that $r > 10^5$.

For an even lighter shadow Higgs, the stellar energy lost through $e\gamma \rightarrow eH_1$ puts a stronger bound on the electron-shadow Higgs Yukawa coupling, $(y_{eH_1}^2)/4\pi \leq 10^{-29}$ [28]. But this would push our model into an extremely fine-tuned region, where $r \geq 10^{16}$.

Recall that $r > 10^4$ is already necessary when considering the rare $B \rightarrow \mu^+\mu^-X$ decay. In this region, if the shadow Higgs is lighter than $0.1 r^{1/3}$ eV, which is 2.15 eV for $r = 10^4$ and 215 eV for $r = 10^{10}$, it can have a cosmologically interesting life time and may contribute a noticeable fraction to the dark matter density. Note that this does not require one to impose a discrete symmetry such as an extra Z_2 parity as in Ref. [17].

E. Searching for the shadow Higgs at the LHC

As can be seen from (35), the 2-body decay widths of the SM-like Higgs H_2 are simply that of the SM scaled by a factor $n_2^2 = r/(1+r)$, and so no significant changes are expected here. More interesting are the 3-body decays described in Fig. 7, whose amplitude is given by

$$\mathcal{M} = \frac{y_f \lambda_3 v_r}{(P-k)^2 - m_{H_2}^2} \bar{u}(l) v(q), \quad \lambda_3 \equiv 4\kappa\sqrt{1+r}, \quad (54)$$

where y_f is the SM Higgs-fermion Yukawa coupling, and $-\lambda_3 v_r/2$ is the coupling of the $H_2 H_2 H_1$ vertex. From a standard calculation, and the fact that the b -quark is much lighter than the SM Higgs, the decay width reads

$$\Gamma(H_2 \rightarrow H_1 f \bar{f}) = N_c \frac{y_f^2 \lambda_3^2}{128\pi^3} \frac{v_r^2}{m_{H_2}} F_H(\beta), \quad (55)$$

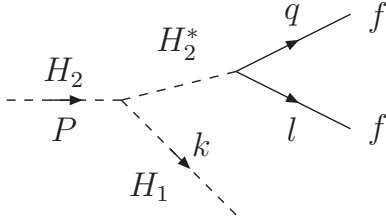


FIG. 7: Leading order 3-body $H_2 \rightarrow H_1 f \bar{f}$ decay.

where

$$F_H(\beta) = \int_{2\beta}^{1+\beta^2} dx \frac{1 + \beta^2 - x}{(x - \beta^2)^2} \sqrt{x^2 - 4\beta^2}, \quad x = \frac{2k_0}{m_{H_2}}, \quad \beta = \frac{m_{H_1}}{m_{H_2}},$$

$$\sim -2 - \log \beta + \frac{5\pi}{4}\beta + \mathcal{O}(\beta^2), \quad 0 < \beta \ll 1. \quad (56)$$

We have thus

$$\sum_f \Gamma(H_2 \rightarrow H_1 f \bar{f}) = \frac{\lambda_3^2}{64\pi^3 m_{H_2}} F_H(\beta) \sum_f N_c m_f^2 \sim 0.3 \lambda_3^2 F_H(\beta) \left(\frac{120 \text{ GeV}}{m_{H_2}} \right) \text{ MeV}, \quad (57)$$

where the sum runs over b, c and τ .

The inclusive width given in (57) is to be compared with $\Gamma_{total} \sim 40$ MeV for a SM Higgs of 120 GeV. Table I lists the relevant quantities entering into (57) for $m_{H_2} = 120$ GeV, $m_{Z_s} = 500$ GeV and $m_{H_1} = 0.001, 1, 30$ GeV. We see that the tree-level $H_2 H_2 H_1$ coupling (in units of v_r) is tiny in all cases. Thus, we expect the 3-body decay process, $H_2 \rightarrow H_1 f \bar{f}$, to have little impact on the branching ratios of the SM-like H_2 .

TABLE I: Values of F_H and λ_3 at various m_{H_1} for $m_{H_2} = 120$ GeV and $m_{Z_s} = 500$ GeV.

m_{H_1} (GeV)	0.001	1	30
F_H	9.96	2.82	0.168
λ_3	-1.4×10^{-6}	-1.4×10^{-3}	-0.04

Since the Yukawa coupling of the top to the SM Higgs is the largest amongst the fermions, it would also be the largest fermion-shadow Higgs coupling as well. Thus we expect that there is a good chance of detecting the shadow Higgs in precision top decay studies such as at the LHC, where $8 \times 10^6 t\bar{t}$ events per year are expected at a luminosity of $10^{33} \text{ cm}^{-2} \text{ s}^{-1}$ [29].

As is the case with the SM Higgs search at the LHC, the primary process that can reveal the presence of the shadow Higgs is the 3-body decay, $t \rightarrow H_1 b W^+$, described in Fig. 8.

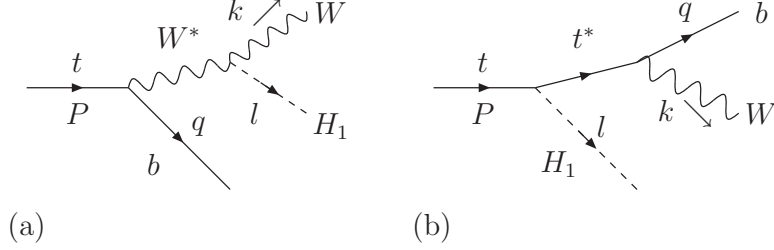


FIG. 8: Leading order 3-body $t \rightarrow H_1 b W^+$ decay.

Taking $m_t = 174$ GeV, $m_W = 80.4$ GeV, $m_b = 4.5$ GeV, and $y_t \sim 1.0$, after a standard but tedious calculation the decay width is evaluated to be

$$\Gamma(t \rightarrow H_1 b W^+) \sim \{16.85, 4.78, 0.221\} \times \frac{\sqrt{2}G_F m_t^3}{256\pi^3} \frac{1}{1+r} \sim \{18, 5, 0.2\} \times \frac{10^{-2}}{1+r} \text{ GeV}, \quad (58)$$

for $m_{H_1} = 0.001, 1, 30$ GeV respectively. This is to be compared with the top decay width predicted in the SM [30]

$$\Gamma_t = \frac{G_F M_t^3}{8\pi\sqrt{2}} (1 - \eta^2)^2 (1 + 2\eta^2) \left[1 - \frac{2\alpha_s}{3\pi} \left(\frac{2\pi^2}{3} - \frac{5}{2} \right) \right] = 1.37 \text{ GeV}, \quad (59)$$

where $\eta = m_W/m_t$ and $\alpha_s(m_Z) = 0.118$.

Suppose that $m_{H_1} = 30$ GeV, $r \simeq 10$, and the experimental sensitivity can reach down to 10^{-4} (which is expected from the LHC at high luminosity), then (58) suggests that the presence of the shadow Higgs can be tested by studying the top decay width. However, as discussed before, the parameter space for having $r \simeq 10$ is small. From Fig. 2(b), we see that for $m_{Z_s} > 500$ GeV, $g_s > 1$ is required, and so the use of perturbation theory becomes questionable. Only for $m_{Z_s} < 300$ GeV can a perturbative g_s be easily maintained. Since r is more naturally of $\mathcal{O}(100)$, a search for the shadow Higgs may require the LHC to operate at high luminosity for extended periods of time.

V. SUMMARY

We have studied the scale invariant version of a hidden extra $U(1)$ model with radiative gauge symmetry breaking. The dimensional transmutation mechanism results in a heavy scalar which we identify as the SM Higgs (H_2), and a light scalon which we call the shadow Higgs (H_1). There are no other physical spin-0 particle in the model.

Unlike other extended Higgs models, there is no tree level $H_2 H_1 H_1$ couplings. Thus, the model predicts no additional two body decays for H_2 , and to leading order, the SM Higgs

physics is only modified by a factor of $r/(1+r)$. As for the shadow Higgs, it behaves in general like a lighter version of the SM Higgs with couplings to quarks and gauge bosons reduced by a factor of $1/(1+r)$. Phenomenological considerations from LEP constraints dictate that $r > 10$ for $m_{H_1} < 100$ GeV.

For a shadow Higgs with mass in the range $2m_e < m_{H_1} < 1$ GeV, the most stringent constrain comes from the $B \rightarrow \mu^+ \mu^- X$ decay that leads to a lower limit of $r > 10^4$. For $m_{H_1} < 20$ keV, stellar cooling imposes the limit of $r > 10^5$. While not impossible, this stretches the limit of fine tuning. For a cosmologically interesting shadow Higgs, $r > 10^6$ would be required.

Given that the coupling of the shadow Higgs to SM particles will be quite weak, the shadow Higgs will be elusive to most searches. However, if its mass is in the range of a few to 100 GeV, it can be detected in top decays. In particular, there will a parallel mode alongside the $t \rightarrow H_2 W b$ decay in which the SM-like Higgs is replaced by the lighter shadow Higgs. If $r \simeq 10$, we expect a branching ratio of $\mathcal{O}(10^{-4})$ for the shadow Higgs, which should be detectable at the LHC with high luminosity runs. In the event that the SM-like Higgs is heavier than or is too close to m_t so that the decay is kinematically suppressed, the shadow Higgs will be the only such decay to be seen. This search can be extended to the ILC where the environment will be much cleaner.

VI. ACKNOWLEDGEMENTS

The research of J.N.N. and J.M.S.W. are partially supported by the Natural Science and Engineering Council of Canada. The research of W.F.C. is supported by Taiwan NSC under grant 95-2112-M-007-032.

-
- [1] R. Schabinger and J. D. Wells, Phys. Rev. D **72**, 093007 (2005).
 - [2] S. Chang, P. J. Fox and N. Weiner, JHEP **0608**, 068 (2006).
 - [3] M. J. Strassler and K. M. Zurek, arXiv:hep-ph/0604261.
 - [4] B. Patt and F. Wilczek, arXiv:hep-ph/0605188.
 - [5] A. V. Manohar and M. B. Wise, Phys. Rev. D **74**, 035009 (2006).
 - [6] D. G. Cerdeno, A. Dedes and T. E. J. Underwood, JHEP **0609**, 067 (2006).

- [7] D. O'Connell, M. J. Ramsey-Musolf and M. B. Wise, arXiv:hep-ph/0611014.
- [8] O. Bahat-Treidel, Y. Grossman and Y. Rozen, arXiv:hep-ph/0611162.
- [9] K. A. Meissner and H. Nicolai, arXiv:hep-th/0612165.
- [10] J. R. Espinosa and M. Quiros, arXiv:hep-ph/0701145.
- [11] see, e.g. R. W. Robinett and J. L. Rosner, Phys. Rev. D **25**, 3036 (1982), D **27**, 679 (1983) (**E**); P. Langacker, R. W. Robinett and J. L. Rosner, Phys. Rev. D **30**, 1470 (1984); F. Zwirner, Int. J. Mod. Phys. A **3**, 49 (1988).
- [12] J. Erler and P. Langacker, Phys. Lett. B **456**, 68 (1999).
- [13] T. Appelquist, B. A. Dobrescu and A. R. Hopper, Phys. Rev. D **68**, 035012 (2003).
- [14] J. Kumar and J. D. Wells, Phys. Rev. D **74**, 115017 (2006).
- [15] W. F. Chang, J. N. Ng and J. M. S. Wu, Phys. Rev. D **74**, 095005 (2006).
- [16] R. Barbieri, L. J. Hall and V. S. Rychkov, Phys. Rev. D **74**, 015007 (2006).
- [17] V. Silveira and A. Zee, Phys. Lett. B **161**, 136 (1985); C. Boehm and P. Fayet, Nucl. Phys. B **683**, 219 (2004).
- [18] S. R. Coleman and E. Weinberg, Phys. Rev. D **7**, 1888 (1973).
- [19] R. Hempfling, Phys. Lett. B **379**, 153 (1996).
- [20] R. Barate *et al.* [LEP Working Group for Higgs boson searches], Phys. Lett. B **565**, 61 (2003).
- [21] E. Gildener and S. Weinberg, Phys. Rev. D **13**, 3333 (1976).
- [22] In preparation.
- [23] P. D. Acton *et al.* [OPAL Collaboration], Phys. Lett. B **268**, 122 (1991).
- [24] J. F. Gunion, H. E. Haber, G. L. Kane and S. Dawson, *The Higgs Hunter's Guide*, Perseus Books Group, 2000.
- [25] D. W. Hertzog, arXiv:hep-ex/0611025.
- [26] W. M. Yao *et al.* [Particle Data Group], J. Phys. G **33**, 1 (2006).
- [27] K. Zioutas *et al.* [CAST Collaboration], Phys. Rev. Lett. **94**, 121301 (2005).
- [28] G. G. Raffelt, *Stars As Laboratories For Fundamental Physics: The Astrophysics Of Neutrinos, Axions, And Other Weakly Interacting Particles*, Chicago Univ. Pr., Chicago, 1996.
- [29] ATLAS: Detector and physics performance technical design report, Volume 1, CERN-LHCC-99-14.
- [30] M. Jezabek and J. H. Kuhn, Nucl. Phys. B **314**, 1 (1989).